

Multipulse Analysis of Adaptive Detection of MTI Radar System in the Presence of Interferers

Mohamed Bakry El Mashade

Electrical Engineering Dept., Faculty of Engineering, Al Azhar University, Nasr City, Cairo, Egypt.
Email: mohamed.b.elmashade@azhar.edu.eg

Abstract. The detection of a moving target against clutter background represents one of the most important goals of a radar system. To satisfactory achieve this objective, it is necessary to suppress or cancel the clutter returns with as small suppression of the target signal as possible. Moving target indication (MTI) radar is capable of detecting such type of targets in the presence of an interfering background. Radar MTI reduces the returns from stationary or slowly moving clutter. In addition to MTI processing, automatic detection may be applied in order to make decisions on the target presence. In this regard, the CFAR detection is a common form of adaptive algorithm used in radar systems to detect target returns against a background of noise, clutter and interference. However, the presence of MTI complicates the analysis of the detection system performance since its output sequence is correlated even though its input sequence may be uncorrelated. Our goal in this paper is to analyze the performance of a radar signal processor that consists of a non-recursive MTI followed by a square-law integrator and a new version of CFAR circuit detection; the operation of which is based on the hybrid combination of CA and TM algorithms. The processor performance is evaluated for the case where the background environment is assumed to be ideal (homogeneous) as well as in the presence of outlying target returns amongst the contents of the reference window. The numerical results show that there is an enhancement in the processor performance when either the number of incoherently integrated pulses increases or the correlation between consecutive sweeps decreases, given that the false alarm rate is held constant.

Keywords: Adaptive detection, moving target indicator (MTI), noise and clutter, developed detectors, incoherent integration of M pulses, multitarget environments.

1 Introduction

Owing to its great versatility, the radar would certainly be a serious, if not the most serious, candidate in the world of instruments which most extends the immense capacities of the human senses. With the radar, one can see in the dark, measure the speed of a moving object precisely, measure the distance of a rain storm or the density of clouds, prevent collisions, obtain advance warning of an impending danger, land in dense fog, determine the relief of mountains, and much more. In other words, radars allow men to do with electromagnetic waves what they would like to be able to do using their senses. Therefore, radars are used almost everywhere. Once one has understood their capabilities, radars can no longer be ignored since they are powerful tools that represent an extension of our capacity to perceive complex situations [1-5].

Target detection is the basic important task that a radar system performs. This task is achieved by emitting electromagnetic waves to illuminate the environment in which the radar operates. It is well-known that if an electromagnetic wave encounters sudden change in conductivity, permittivity or permeability in the medium, a part of the electromagnetic energy gets absorbed by the second medium and is reradiated. The sudden change in the electrical property of the medium constitutes the target. The detection is realized by observing the nature of the received echo from the physical objects that may be found in the operating environment. The detection itself is fairly straightforward. It compares the signal to a threshold. Therefore, the real work on detection is coming up with an appropriate threshold. In general, the threshold is a function of both the probability of detection and the probability of false alarm. Because of the cost associated with a false detection, it is desirable to have a detection

threshold that not only maximizes the probability of detection but also keeps the probability of false alarm below a preset level [6-9].

Clutter is the major problem for outdoor radar operations and there is no standard measure to reject it. The nature of clutter varies with application and radar parameters because of many users and the over-crowding of the spectrum. Electromagnetic interference is a common occurrence with current communication and electronic equipments. Hence, avoidance or elimination of such interference is of primary concern of the radar designer. One of the most efficient methods for doing this is to exploit the Doppler shift in reflections from moving targets. This is called moving target indication (MTI), and it is used in many radar applications today. Ideally, clutter components will be removed by the MTI process, leaving receiver noise and reflection from targets at the output. The MTI signal exhibits spatial correlation between clutter samples. The correlation is concluded to be the reason for degradation in performance, as detection on clutter appears as targets. In addition to MTI processing, automatic detection may be applied in order to make decisions on target presence. This may be achieved by employing constant false alarm rate (CFAR) detection and pulse integration. The challenges with automatic detection are prediction of the clutter power, and handling of non-homogeneous environments. In modern radar systems, equipped with automatic detection circuits, the use of CFAR techniques is required to keep false alarms at a suitably low rate in an a priori unknown time varying and spatially non-homogeneous environments. One of the main tasks of CFAR detectors is to avoid the radar performance impairment when it operates in target multiplicity environments. As a consequence, much attention has been paid to the task of designing and assessing of this type of adaptive detection systems. The threshold in these detectors is set adaptively based on the estimation of the noise power level. This is because the noise power is not known a priori and a fixed threshold value may increase the false alarm probability to a much higher value than the required one or decrease the detection probability intolerably [10].

In the CFAR world, the CA algorithm is the CFAR method with highest detection probability in homogeneous backgrounds. However, it exhibits poor performance when a clutter edge or multiple targets are present. As the latter is often encountered in maritime environments, one may look towards other CFAR methods. The order-statistics (OS) procedure has worse performance in homogeneous environments than the CA scheme, but is clearly superior in the presence of clutter edges and multiple targets. A more generalized OS scheme which combines ordering with arithmetic averaging is known as trimmed mean (TM). Recently, a new CFAR algorithm named (CATM), which is a combination of CA- and TM-CFAR, has been appeared [11]. This version of CFAR schemes has some merits over other types of CFAR procedures. When considering MTI processed radar signals, one would assume that a great part of the clutter components would have been removed, and that clutter edges would not occur unless it moves with a Doppler velocity larger than the MTI threshold. Situations with multiple targets are more likely to be encountered, and it is desired to have a robust CFAR detector that is able to deal with such situations. The objective of this manuscript is to analyze the novel version of automatic detection of radar signals after MTI processing. The radar receiver is assumed to be a non-recursive MTI followed by a square-law integrator that integrates M pulses to form the input of the CFAR circuit. The remainder of this paper proceeds as follows. Section II contains the detector description and the formulation of the problem under consideration. The processor performance is analyzed in section III. Our numerical results that illustrate the effects of the detector parameters on its performance in the absence as well as in the presence of extraneous targets are displayed in section IV. Finally, our concluding remarks are provided in Section V.

2 Problem Formulation

In the radar receiver the returning echoes are typically received by the antenna, amplified, down-converted and then passed through detector circuitry that extracts the envelope of the signal which is known as the video signal. The resulting video signal is proportional to the power of the received echo and comprises the wanted echo signal along with the unwanted power from internal receiver noise and external clutter and interference. One of the most important goals of a radar system is to detect a moving target against clutter. To carry out this task, it is necessary to suppress or cancel the clutter returns with as small suppression of the target signal as possible. One of the most efficient methods for

doing this is to exploit the Doppler shift in reflections from moving targets. This is called moving target indication (MTI), and it is used in many radar applications today. In other words, MTI is the process of rejecting fixed or slowly moving clutter while passing echoes from targets moving at significant velocities [5,6,8].

The detection of moving targets is achieved, through MTI processor, by performing a high pass filtering process. The weights of the filter taps are chosen in such a way that the resulting transfer function of the MTI attenuates the input signal power at frequencies where the clutter return is dominant. This is accomplished by coherently subtracting each range gate return from a delayed version of the previous echo from the same range gate. If nothing has changed, cancellation of clutter signal occurs which would be complete in the absence of noise. If, on the other hand, the echo has slightly phase changed, because of its motion, the cancellation will be less complete [12].

The inclusion of MTI as a fundamental element amongst the contents of the detection system complicates the analysis of its performance since its output sequence is correlated even if its input sequence is not [4]. The objective of this research is to handle this problem. For this situation, the MTI outputs are quadratically detected and M consecutive of these outputs ~~are~~ are incoherently integrated to provide the input to the adaptive scheme. The MTI considered here is of a non-recursive type of digital filters that linearly combined the inputs h_i 's from M successive pulse repetition intervals in such a way that the l th component of its output x has a form given by

$$x_\ell = W^T H^{(\ell)} \tag{1}$$

In the above expression, W & H denote M -component vectors defined as

$$W^T \triangleq [w_1, w_2, w_3, \dots, w_M] \quad \& \quad H^{(\ell)} \triangleq [h_\ell, h_{\ell-1}, h_{\ell-2}, \dots, h_{\ell-M+1}]^T \tag{2}$$

In the above expression, the letter T over a specified vector stands for vector transposition.

The fixed weights w_i 's applied to the filter taps are selected in an optimum way that attenuates the dominant clutter return signal components. The input samples h_j 's are assumed to be mutually independent white Gaussian random sequence with mean μ_j and variance σ^2 . According to the central limit theory, the sequence x_ℓ becomes Gaussian, the mean and covariance of which are [8]:

$$\bar{x}_\ell \triangleq E \{ x_\ell \} = W^T \mu^{(\ell)}, \mu^{(\ell)} \triangleq [\mu_\ell, \mu_{\ell-1}, \mu_{\ell-2}, \dots, \mu_{\ell-M+1}]^T \tag{3}$$

with E symbolizes the expectation operator and

$$E \{ x_\ell x_{\ell+m} - \bar{x}_\ell \bar{x}_{\ell+m} \} = \begin{cases} \sigma^2 \sum_{i=1}^{M-m} w_i w_{i+m} & \text{for } |m| < M \\ 0 & \text{for } |m| \geq M \end{cases} \tag{4}$$

Similarly, if the input sequence g_ℓ 's to the quadratic MTI has the same variance as the inphase channel and with mean ν_ℓ , its output sequence y_ℓ has a normal distribution with mean and covariance of the same forms as those given in Eqs.(3-4). Moreover, the two resulting sequences x_ℓ and y_ℓ are uncorrelated. Thus,

$$E \{ x_\ell y_{\ell+m} - \bar{x}_\ell \bar{y}_{\ell+m} \} = 0 \tag{5}$$

The set of Eqs.(1-5) represents the basic theoretical background of the MTI processor treated in this research.

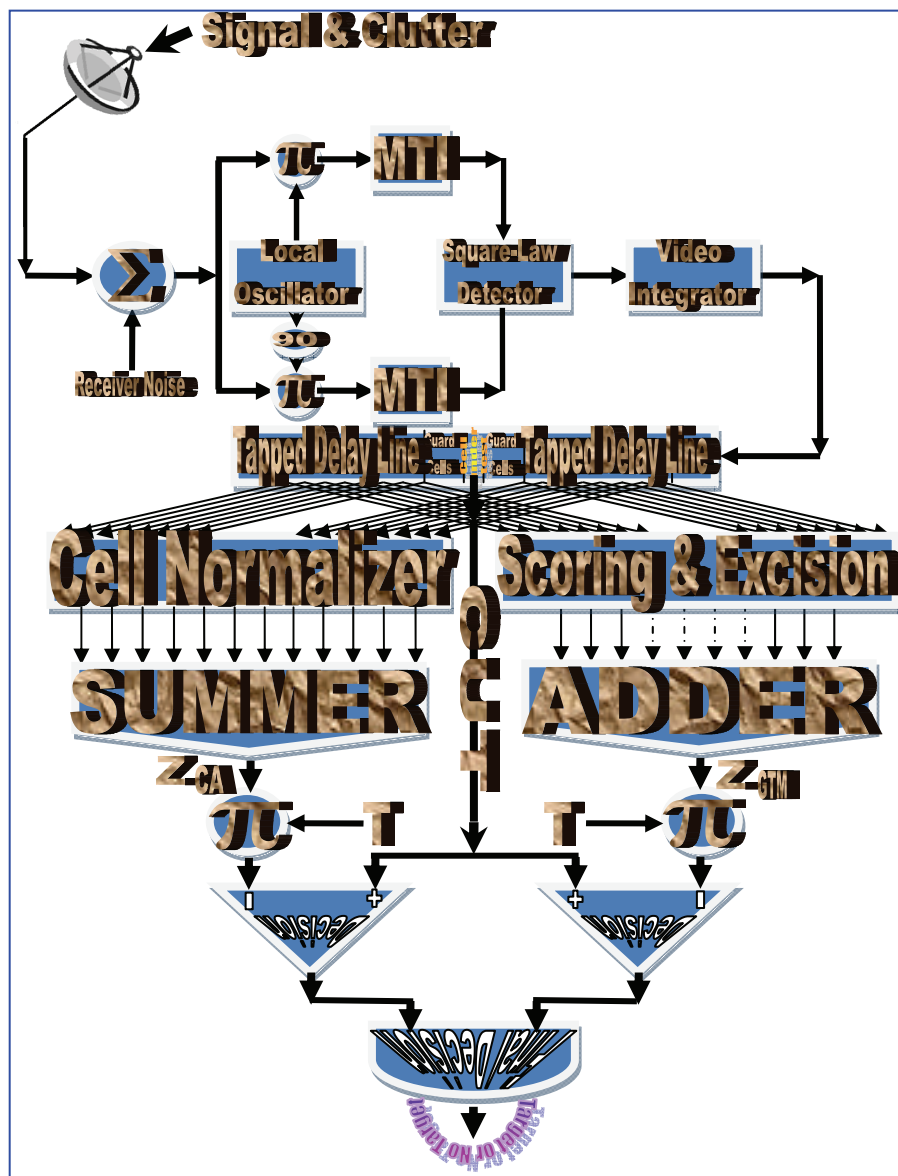


Figure 1. Architecture of MTI radar receiver with CA_GTM adaptive threshold scheme

MTI and automatic detection may be combined after the matched filter. In this regard, automatic detection is applied after the introduction of MTI processing in order to make decision on the target presence. In this situation, it is of importance to note that MTI utilizes the phase information, whilst automatic detection uses the magnitude. The role of the CFAR circuitry is to determine the power threshold above which any return can be considered to probably originate from a target. If the background against which targets are to be detected is constant with time and space, then a fixed threshold level can be installed to provide a specified probability of false alarm, governed by the statistical properties noise. This is rarely the case where the background clutter changes due to the non-stationary characteristics of operating environments. Therefore, the CFAR strategy replaces the fixed-threshold algorithm to update its threshold in such a way that it follows the clutter variations. In most simple CFAR detection schemes, the threshold level is calculated by estimating the level of the noise floor around the cell under test (CUT). To avoid corrupting this estimate with power from the CUT itself, cells immediately adjacent to the CUT, guard cells, are normally ignored. More sophisticated CFAR algorithms can adaptively select a threshold level by taking a rigorous account of the statistics of the background in which targets are to be detected. The CA detector is probably the most widely used

CFAR detector. It is also used as a baseline comparison for other CFAR techniques. Recently, the cell-averaging-trimmed-mean (CATM) CFAR scheme has been appeared [11]. It optimizes good features of some well-known CFAR processors. It is realized by parallel operation of CA and TM algorithms. These familiar schemes operate simultaneously and independently but with the same scaling factor of the detection threshold T . They produce their own mean clutter power levels, Z_{CA} & Z_{TM} , using their appropriate technique of CFAR. Next, they compute their own detection thresholds and finally they independently achieve their decision about the target presence. This CFAR detection scheme is depicted in Fig.(1). Scientifically, it is known that when several detectors are employed simultaneously, as could arise in the weak signal case, a fusion algorithm is used to arrive at a global decision. Based on this rule, the finite decision about target presence is made in fusion center which is composed of an AND logic gate. If both the input single decisions to the fusion center are positive, the global decision of the fusion center is the target presence in the content of the CUT. In each output of other cases, finite decision is negative and the target is absent at the location which corresponds to the tested cell. In other words, the decision hypotheses can be adaptively constructed according to the relation:

$$\beta \begin{matrix} \text{TARGET PRESENT} \\ \rangle \\ \langle \\ \text{TARGET ABSENT} \end{matrix} \quad V_T \ \& \ V_T \triangleq TZ_{CA} \wedge TZ_{TM} \quad (6)$$

In the previous stated formula, β represents the content of the CUT, V_T stands for the detection threshold, Z_{CA} & Z_{TM} designate the background noise power levels estimated through CA and TM rules, respectively, T denotes the constant scale factor chosen in such a way that it adjusts the false alarm to satisfy the pre-assigned level when the radar operates in an ideal (homogeneous) environment, and \wedge symbolizes the algebraic Boolean of AND gate. After this general insight of the CFAR world, let us go to formulate our interesting problem.

After extracting the baseband signal by the square-law detector, M -consecutive sweeps with sweep-to-sweep correlation coefficient ρ are incoherently integrated to improve the received SNR and correspondingly the detection probability. This integrated form of the received signal is then processed by the CFAR circuit. The integrator output is firstly sampled and the sampling rate is assumed to be such that the successive samples are statistically independent. A set of N samples is picked up from each sweep to construct the basics of noise level estimation. Noise samples are assumed to be independent within a specified sweep while they are correlated from one sweep to another. This situation is similar to that processed by some radar and sonar systems in which the time and frequency axes would represent delay and Doppler shift. On the other hand, this problem can be fitted to diversity communication through a noisy channel. To mathematically formulate this problem, let Λ denotes the matrix of data to be processed. The rows of this matrix represent the reference samples belong to each sweep, while its columns denote the number of pulses to be incoherently integrated. As a consequence of this organization, the resulting matrix has an $M \times (N+1)$ dimension, which can be formulated as:

$$\Lambda \triangleq \begin{bmatrix} q_{1(-\frac{N}{2})} & q_{1(-\frac{N}{2}+1)} & \cdots & q_{1(-1)} & q_{10} & q_{11} & \cdots & q_{1(\frac{N}{2}-1)} & q_{1(\frac{N}{2})} \\ q_{2(-\frac{N}{2})} & q_{2(-\frac{N}{2}+1)} & \cdots & q_{2(-1)} & q_{20} & q_{21} & \cdots & q_{2(\frac{N}{2}-1)} & q_{2(\frac{N}{2})} \\ \cdots & \cdots \\ \vdots & \vdots & \cdots & \vdots & \vdots & \vdots & \cdots & \vdots & \vdots \\ \cdots & \cdots \\ \vdots & \vdots & \cdots & \vdots & \vdots & \vdots & \cdots & \vdots & \vdots \\ q_{M(-\frac{N}{2})} & q_{M(-\frac{N}{2}+1)} & \cdots & q_{M(-1)} & q_{M0} & q_{M1} & \cdots & q_{M(\frac{N}{2}-1)} & q_{M(\frac{N}{2})} \end{bmatrix} \quad \& \quad q_{i\ell} \triangleq x_{i\ell} + jy_{i\ell} \quad (7)$$

Integration means that the elements of each column are added up. Let the random variable (RV) describing the addition of the elements of the ℓ th column be denoted by α_ℓ while that representing the sum of the column under test be indicated as β . Therefore,

$$\alpha_\ell \triangleq \sum_{k=1}^M |q_{k\ell}|^2 = \sum_{k=1}^M x_{k\ell}^2 + y_{k\ell}^2 \quad \& \quad -\frac{N}{2} \leq \ell \leq -1, \quad 1 \leq \ell \leq \frac{N}{2} \quad (8)$$

and

$$\beta \triangleq \sum_{\ell=1}^M |q_{\ell 0}|^2 = \sum_{\ell=1}^M x_{\ell 0}^2 + y_{\ell 0}^2 \tag{9}$$

In the above expression, x_{ij} and y_{ij} denote the inphase and quadrature MTI outputs. Since the output sequence of MTI is correlated, the RV's $q_{k\ell}$ are correlated. Generally, for M -consecutive sweeps with sweep-to-sweep correlation coefficient $\rho_{k\ell}$, the correlation matrix of the integrator output takes the form [5]:

$$\Theta \triangleq \begin{bmatrix} 1 & \rho_{12} & \rho_{13} & \rho_{14} & \dots & \dots & \dots & \rho_{1M} \\ \rho_{21} & 1 & \rho_{23} & \rho_{24} & \dots & \dots & \dots & \rho_{2M} \\ \rho_{31} & \rho_{32} & 1 & \rho_{34} & \dots & \dots & \dots & \rho_{3M} \\ \rho_{41} & \rho_{42} & \rho_{43} & 1 & \dots & \dots & \dots & \rho_{4M} \\ \dots & \dots \\ \dots & \dots \\ \dots & \dots \\ \rho_{M1} & \rho_{M2} & \rho_{M3} & \rho_{M4} & \dots & \dots & \dots & 1 \end{bmatrix} \quad \& \quad 0 \leq \rho_{k\ell} \leq 1 \tag{10}$$

Through the orthogonal transformation, the above matrix can be diagonalized by solving its associated eigenvalue problem. The resulting eigenvalues of this processing determine the interferences, whilst the developed eigenvectors provide the signal gains. In terms of these interesting signal parameters, the moment generating function (MGF) of the integrator output for the CUT β , which is more general than the noise only cell, has a form given by [6]

$$\Omega_{\beta}(S) = \left\{ \prod_{\ell=1}^M (1 + \psi \lambda_{\ell} S) \left[1 + \eta \left(\sum_{j=1}^M \frac{G_j}{1 + \psi \lambda_j S} \right) S \right] \right\}^{-1} \tag{11}$$

where

$$G_j \triangleq \sum_{k=1}^M \sum_{\ell=1}^M A_k^{(j)} A_{\ell}^{(j)} \tag{12}$$

and

$$\eta \triangleq \begin{cases} 0 & \text{FOR CLEAR BACKGROUND} \\ \psi I & \text{FOR OUTLYING TARGET} \\ \psi \gamma & \text{FOR PRIMARY TARGET} \end{cases} \tag{13}$$

In the above formulas, λ_j , $A^{(j)}$, and G_j denote the j th eigenvalue, the corresponding eigenvector and its associated signal gain, respectively. ψ represents the total clutter-plus-thermal noise power, I and γ designate the interference-, and signal-to-noise ratios (INR & SNR), respectively. This means that the returns from the spurious as well as the primary target follow Swerling I (SWI) model in their fluctuation [13].

Let us now go to formulate the basic rules which distinguish one CFAR processor from the other. These rules are the probabilities of detection and false alarm. Our starting point to attain this goal is the MGF given in Eq.(11). This function is derived for the case where the RV's $|q_{k0}|^2$ are correlated and identically distributed, each with probability density function (PDF) of exponential form as:

$$p_{\beta}(\beta) = \frac{1}{\xi} \exp\left(-\frac{\beta}{\xi}\right) U(\beta) \tag{14}$$

$U(\cdot)$ stands for the unit-step function and ξ denotes the parameter for which the exponential distribution is defined. This parameter can take several forms according to its origin as:

$$\xi \triangleq \begin{cases} \psi & \text{FOR CLEAR BACKGROUND SAMPLE} \\ \psi(1 + I) & \text{FOR INTERFERING TARGET RETURN} \\ \psi(1 + \gamma) & \text{FOR TESTING TARGET RETURN} \end{cases} \tag{15}$$

In order to simplify the required calculation, it is intuitive to obtain the time-domain representation of Eq.(11). To carry out this inverse, Eq.(11) can be formulated in an M th order polynomial in S as:

$$\Omega_{\beta}(S) = \left\{ \sum_{k=0}^M \zeta_k S^k \right\}^{-1} \tag{16}$$

The coefficients ζ_i 's are functions of λ_j , $A^{(j)}$, G_j , and η . If the roots of this M th order polynomial are known, either analytically or numerically, the PDF corresponding to this MGF can be easily obtained. Letting ω_j 's, $j=1, 2, \dots, M$, denote these roots, Eq.(16) can be written as a function of them as:

$$\Omega_{\beta}(S) = \prod_{\ell=1}^M \frac{\omega_{\ell}}{S + \omega_{\ell}} \tag{17}$$

The Laplace inverse of the above formula yields:

$$p_{\beta}(\beta) = \sum_{j=1}^M \varepsilon_j \exp(-\omega_j \beta) \tag{18}$$

The coefficients ε_j 's of the exponential terms are functions of the roots ω_j 's, where:

$$\varepsilon_j \triangleq \omega_j \prod_{\substack{\ell=1 \\ \ell \neq j}}^M \frac{\omega_{\ell}}{\omega_{\ell} - \omega_j} \tag{19}$$

In deriving the above expression, it is assumed that all the poles of $\Omega_{\beta}(\cdot)$ are simple. However, if there are some repetitive poles, the PDF of β can be easily obtained through the technique of partial fraction method. A detector's performance is measured by its ability to achieve a certain probability of detection for a given SNR as well as a specified rate of false alarm. The processor detection performance can be evaluated from the well known relation [14]

$$P_d = \int_0^{\infty} p_{\beta}(\beta / \gamma) F_Z(\beta / T) d\beta \tag{20}$$

In the above expression, $p_{\beta}(\cdot)$ denotes the PDF of the CUT, $F_Z(\cdot)$ designates the cumulative distribution function (CDF) of the noise level estimate Z . The substitution of Eq.(18) into Eq.(20) yields:

$$P_d = \sum_{\ell=1}^M \varepsilon_{\ell} \int_0^{\infty} F_Z(\beta / T) \exp(-\omega_{\ell} \beta) d\beta = T \sum_{\ell=1}^M \varepsilon_{\ell} \Psi_Z(s) \Big|_{s=T \omega_{\ell}} \tag{21}$$

$\Psi_Z(\cdot)$ represents the Laplace transformation of the CDF of the noise level estimate Z . From this relation, it is evident that the backbone of our analysis is the evaluation of the roots of the MGF of the CUT variate along with the determination of the Laplace transformation of the CDF of the background noise level. This is actually what we will go to do in the next section for the detection performance of the underlined adaptive scheme to be completely analyzed.

3 Processor Performance Analysis

The key assumption in the tested CFAR algorithm is that the reference cell variates have the same distribution as that of the CUT variate in the no target present case. The sliding window is constructed by collecting N variates α_{ℓ} 's, $-N/2 \leq \ell \leq -1$ for the trailing sub-window, whilst $1 \leq \ell \leq N/2$ for the leading one. Thus, we have

$$Q_1 \xleftarrow{\text{Lagging}} \alpha_k, -\frac{N}{2} \leq k \leq -1 \ \& \ Q_2 \xleftarrow{\text{Leading}} \alpha_j, 1 \leq j \leq \frac{N}{2} \tag{22}$$

These samples are statistically independent and identically distributed (IID) random variables, as it was previously stated. Since the non-homogeneous case is the more general situation, it is preferable to analyze the performance of the examined detectors for the case where the reference window no longer contains radar returns from a homogeneous background. The assumption of statistical independence of the reference cells is retained. Suppose the trailing sub-window contains r_1 cells from outlying target returns and $N/2 - r_1$ cells from clear background. Similarly, the leading reference sub-window has r_2 of the interfering returns and $N/2 - r_2$ of the clear background amongst its contents. Taking these postulates into consideration, the estimated total noise power is obtained as:

$$Q_1 \triangleq \sum_{i=1}^{r_1} \alpha_i + \sum_{j=1}^{m_1} \alpha_j, Q_2 \triangleq \sum_{k=1}^{r_2} \alpha_k + \sum_{\ell=1}^{m_2} \alpha_{\ell} \ \& \ m_n \triangleq \frac{N}{2} - r_n, n = 1, 2 \tag{23}$$

The RV's representing returns from clutter background and extraneous targets have MGF of the same form as that given in Eq.(11) after replacing η by its corresponding values according to Eq.(13). Therefore,

$$\Omega_t(s) = \prod_{j=1}^M (1 + \psi \lambda_j s)^{-1} \quad (24)$$

and

$$\Omega_o(s) = \left\{ \prod_{j=1}^M (1 + \psi \lambda_j s) \left[1 + \psi I \left(\sum_{i=1}^M \frac{G_i}{1 + \psi \lambda_i s} \right) s \right] \right\}^{-1} \quad (25)$$

To simplify our analysis, Eqs.(24-25) can be formulated in a more simpler form as that given in Eq.(17). Thus,

$$\Omega_t(s) = \prod_{\ell=1}^M \frac{a_\ell}{s + a_\ell} \quad \& \quad a_\ell \triangleq \frac{1}{\psi \lambda_\ell} \quad (26)$$

and

$$\Omega_o(s) = \prod_{k=1}^M \frac{b_k}{s + b_k} \quad (27)$$

In the above expressions, b_k 's denote the roots of its associating M th order polynomial of s . The Laplace inverse representations of the above formulas are:

$$p_t(x) = \sum_{j=1}^M \theta_j \exp(-a_j x) \quad \& \quad \theta_j \triangleq a_j \prod_{\substack{i=1 \\ i \neq j}}^M \frac{a_i}{a_i - a_j} \quad (28)$$

and

$$p_o(y) = \sum_{k=1}^M \mathcal{G}_k \exp(-b_k y) \quad \& \quad \mathcal{G}_k \triangleq b_k \prod_{\substack{\ell=1 \\ \ell \neq k}}^M \frac{b_\ell}{b_\ell - b_k} \quad (29)$$

After the formulation of the PDF of the samples belonging to thermal and outlying targets, we are going to analyze the CA, OS, and TM architectures along with their developed versions.

3.1 Cell-Averaging (CA) Procedure

This algorithm estimates the noise variance for the range cell of interest by adding the contents of the two, leading and trailing, sub-windows. As Eq.(23) indicates, the noise level estimate of the trailing sub-window is formulated as Q_1 . Since the two estimate types of Q_1 are statistically independent, its MGF has a mathematical form given by:

$$\Omega_{Q_1}(s) = \left\{ \Omega_t(s) \right\}^{m_1} \left\{ \Omega_o(s) \right\}^{r_1} \quad (30)$$

In the above expression, $\Omega_t(\cdot)$ & $\Omega_o(\cdot)$ are as previously defined in Eqs.(26-27). Similarly, the leading subset has the same form for its MGF as that given by Eq.(30) after replacing m_1 & r_1 by m_2 & r_2 , respectively. Since the two noise level estimates are statistically independent, the final noise level estimate Z_{CA} has the following formulas for its t - and s -domain representations. Thus,

$$Z_{CA} \triangleq Q_1 + Q_2 \quad \& \quad \Omega_{Z_{CA}}(s) = \left\{ \Omega_t(s) \right\}^{m_1+m_2} \left\{ \Omega_o(s) \right\}^{r_1+r_2} \quad (31)$$

As a function of the MGF of the noise power estimate Z_{CA} , the Laplace transformation of its CDF becomes:

$$\Psi_{Z_{CA}}(s) = s^{-1} \Omega_{Z_{CA}}(s) \quad (32)$$

Once the s -domain representation of the CDF of the estimate of the unknown noise power is obtained, the false alarm and detection probabilities can be easily computed as Eq.(21) demonstrates.

3.2 Order-Statistics (OS) Processor

The CA detector is optimum in homogeneous noise or clutter. However, it suffers performance degradation in heterogeneous situations. In order to alleviate this problem, the CA technique is modified by replacing the arithmetic averaging rule by a new data fusion rule based on order statistics technique and the new version is known as OS detector. The OS processor estimates the noise power simply by selecting the K th largest sample in the reference window. This detection scheme suffers only minor degradation in detection probability and resolves closely spaced targets effectively for K different from the maximum. Therefore, the background noise level Z of each subset is estimated by the K th largest cell among the $N/2$ reference ones. Thus, the procedure first ranks the outputs of all reference cells of each sub-window in an ascending order according to their magnitudes in such a way that:

$$D_\ell \triangleq \alpha_{(\ell+1)} - \alpha_{(\ell)} \geq 0 \ \& \ \ell = 1, 2, \dots, N/2 - 1 \tag{33}$$

In this ordered samples, $\alpha_{(1)}$ is the lowest noise level and $\alpha_{(N/2)}$ is the highest level. Next, the K th sample is picked to represent the unknown noise level in each sub-window. Thus,

$$Q_i \triangleq \alpha_{(K_i)}, 1 \leq K_i \leq N/2 \ \& \ i = 1, 2 \tag{34}$$

Aiming at evaluating the performance of the OS algorithm, the PDF of a K th ordered sample out of $N/2$ ones is required when these samples *are* independent, but not identically distributed. Consider the situation where the reference sub-window contains r cells having interfering target returns each with power level $\psi(1+I)$ and the remaining, $m = N/2 - r$, cells contain thermal noise only each with power level ψ . In both cases, the observations are governed by the exponential PDF, see Eqs.(28, 29), and are statistically independent quantities. The expression for the CDF of Q_i in this case has a formula given by [14]:

$$F_Q^{NH}(x; K_\ell, r_\ell) = \sum_{i=K_\ell}^{N/2} \sum_{j=Max(0, i-r_\ell)}^{Min(i, m_\ell)} \binom{m_\ell}{j} \binom{r_\ell}{i-j} \sum_{n=0}^j \binom{j}{n} (-1)^n \sum_{\nu=0}^{i-j} \binom{i-j}{\nu} (-1)^\nu \{1 - F_t(x)\}^{m_\ell-n} \{1 - F_o(x)\}^{r_\ell-\nu} \tag{35}$$

In the above expression, $F_t(\cdot)$ represents the CDF of the cell that contains thermal background only whilst $F_o(\cdot)$ denotes the same thing for the cell that has outlying target return. Under the operating conditions of M -correlated sweeps, these CDF's can be easily obtained since their corresponding PDF's are previously calculated. For thermal noise samples, their associated CDF becomes:

$$F_t(x) \triangleq \int_0^x p_t(u) du = \sum_{k=1}^M \frac{\theta_k}{a_k} [1 - \exp(-a_k x)] = 1 - \sum_{k=1}^M \phi_k \exp(-a_k x) \tag{36}$$

Similarly,

$$F_o(x) \triangleq \int_0^x p_o(u) du = 1 - \sum_{k=1}^M \delta_k \exp(-b_k x) \tag{37}$$

with

$$\phi_j \triangleq \prod_{\substack{i=1 \\ i \neq j}}^M \frac{a_i}{a_i - a_j} \ \& \ \delta_j \triangleq \prod_{\substack{i=1 \\ i \neq j}}^M \frac{b_i}{b_i - b_j} \tag{38}$$

The substitution of Eqs.(36, 37) into Eq.(35) gives:

$$F_Q^{NH}(x; K_\ell, r_\ell) = \sum_{i=K_\ell}^{N/2} \sum_{j=Max(0, i-r_\ell)}^{Min(i, m_\ell)} \binom{m_\ell}{j} \binom{r_\ell}{i-j} \sum_{n=0}^j \sum_{\nu=0}^{i-j} \binom{j}{n} \binom{i-j}{\nu} (-1)^{n+\nu} \left\{ \sum_{\zeta=1}^M \phi_\zeta \exp(-a_\zeta x) \right\}^{m_\ell-n} \left\{ \sum_{\xi=1}^M \delta_\xi \exp(-b_\xi x) \right\}^{r_\ell-\nu} \tag{39}$$

The above formula can be written in another sophisticated version as:

$$\begin{aligned}
 F_Q^{NH}(x; K_\ell, m_\ell, r_\ell) &= \sum_{i=K_\ell}^{N/2} \sum_{j=\text{Max}(0, i-r_\ell)}^{\text{Min}(i, m_\ell)} \binom{m_\ell}{j} \binom{r_\ell}{i-j} \sum_{n=0}^j \sum_{v=0}^{i-j} \binom{j}{n} \binom{i-j}{v} (-1)^{n+v} \\
 &\quad \sum_{v_1=0}^{m_\ell-n} \sum_{v_2=0}^{m_\ell-n} \dots \sum_{v_M=0}^{m_\ell-n} \Xi(m_\ell - n; v_1, v_2, v_3, \dots, v_M) \prod_{\eta=1}^M \phi_\eta^{v_\eta} \exp\left(-\sum_{\varepsilon=1}^M v_\varepsilon a_\varepsilon x\right) \\
 &\quad \sum_{\tau_1=0}^{r_\ell-v} \sum_{\tau_2=0}^{r_\ell-v} \dots \sum_{\tau_M=0}^{r_\ell-v} \Xi(r_\ell - v; \tau_1, \tau_2, \tau_3, \dots, \tau_M) \prod_{\lambda=1}^M \delta_\lambda^{\tau_\lambda} \exp\left(-\sum_{\sigma=1}^M \tau_\sigma b_\sigma x\right)
 \end{aligned} \tag{40}$$

The computation of the s -domain representation of Eq.(40) yields:

$$\begin{aligned}
 \Psi_Q^{NH}(s; K_\ell, m_\ell, r_\ell) &= \sum_{i=K_\ell}^{N/2} \sum_{j=\text{Max}(0, i-r_\ell)}^{\text{Min}(i, m_\ell)} \binom{m_\ell}{j} \binom{r_\ell}{i-j} \sum_{n=0}^j \sum_{v=0}^{i-j} \binom{j}{n} \binom{i-j}{v} (-1)^{n+v} \\
 &\quad \sum_{v_1=0}^{m_\ell-n} \sum_{v_2=0}^{m_\ell-n} \sum_{v_3=0}^{m_\ell-n} \dots \sum_{v_M=0}^{m_\ell-n} \Xi(m_\ell - n; v_1, v_2, v_3, \dots, v_M) \prod_{\eta=1}^M \phi_\eta^{v_\eta} \\
 &\quad \sum_{\tau_1=0}^{r_\ell-v} \sum_{\tau_2=0}^{r_\ell-v} \sum_{\tau_3=0}^{r_\ell-v} \dots \sum_{\tau_M=0}^{r_\ell-v} \Xi(r_\ell - v; \tau_1, \tau_2, \tau_3, \dots, \tau_M) \prod_{\lambda=1}^M \delta_\lambda^{\tau_\lambda} \frac{1}{s + \sum_{\varepsilon=1}^M v_\varepsilon a_\varepsilon + \sum_{\sigma=1}^M \tau_\sigma b_\sigma}
 \end{aligned} \tag{41}$$

In the previous formulas, the term $\Xi(L; \ell_1, \ell_2, \ell_3, \dots, \ell_M)$ is defined as:

$$\Xi(L; \ell_1, \ell_2, \ell_3, \dots, \ell_M) \triangleq \begin{cases} \frac{\Gamma(L+1)}{\prod_{i=1}^M \Gamma(\ell_i + 1)} & \text{if } \sum_{j=1}^M \ell_j = L \\ 0 & \text{if } \sum_{j=1}^M \ell_j \neq L \end{cases} \tag{42}$$

The final noise power level is obtained by combining the two noise level estimates through the mean operation. Thus,

$$Z_f = \sum_{i=1}^2 Q_i(K_i, m_i, r_i) \tag{43}$$

Since the estimates of the background noise level are statistically independent, the MGF of Z_f is simply obtained through the relation:

$$\Omega_{Z_f}(s) = \prod_{\ell=1}^2 \Omega_{Q_\ell}(s; K_\ell, m_\ell, r_\ell) = \prod_{\ell=1}^2 s \Psi_{Q_\ell}(s; K_\ell, m_\ell, r_\ell) \tag{44}$$

As previously stated, once the MGF of the noise level estimate is calculated, the processor detection performance can be easily evaluated as Eqs.(21 & 32) reveal.

3.3 Trimmed-Mean (TM) Procedure

The more generalized form of the OS scheme is what is known as trimmed-mean (TM) procedure. The motivation of using this algorithm is to combine the benefits of averaging and ordering along with censoring. In this scheme, the noise power is estimated by a linear combination of some selected ordered range cells. In the TM-CFAR scheme, the statistic Z_{TM} is obtained by censoring L below ordered range samples and U upper ordered cells before adding the remaining samples to establish such statistic. Thus,

$$Z_{TM}(N, L, U) \triangleq \sum_{k=L+1}^{N-U} \alpha_{(k)} \tag{45}$$

The TM strategy reduces to the conventional CA and OS scenarios for specific trimming values. In other words, $TM(N, 0, 0)$ and $TM(N, K-1, N-K)$ tend to the well-known CA and OS(K) processors, respectively; each handles N reference cells to estimate the unknown noise power level.

Clearly, the ordered samples $\alpha_{(i)}$'s are neither independent nor identically distributed, so the performance evaluation of TM scheme becomes more complicated. To solve this problem, a mathematical transformation is needed. In other words, to make $\alpha_{(i)}$'s meet IID property, a linear transformation of the form:

$$E_\ell \triangleq \alpha_{(L+\ell)} - \alpha_{(L+\ell-1)} U^{(\ell-2)} \tag{46}$$

must be used. As a function of these new variables E_i 's, Eq.(45) can be written as:

$$Z_{TM}(N, L, U) = \sum_{k=1}^{N_T} O_k, O_k \triangleq (N_T - k + 1) E_k \ \& \ N_T \triangleq N - U - L \tag{47}$$

The RV's O_i 's are independent since the RV's E_i 's are independent. As a consequence of this statistical property, the MGF of Z_{TM} can be easily obtained by the product of the individual MGF's of O_i 's. To find the MGF of O_j 's, it is convenient to calculate the MGF of E_j 's. In terms of the s -domain representation of the CDF of the ordered samples $\alpha_{(i)}$'s, the MGF of the random variables E_j 's can be evaluated as [5]:

$$\Omega_{E_\ell}(s; K_i, m_i, r_i) = \begin{cases} s\Psi_{L_i+1}(s; K_i, m_i, r_i) & \text{for } \ell=1 \\ \Psi_{L_i+\ell}(s; K_i, m_i, r_i) / \Psi_{L_i+\ell-1}(s; K_i, m_i, r_i) & \text{for } 1 < \ell \leq N_T \end{cases} \ \& \ i=1,2 \tag{48}$$

After obtaining the formula (48), the computation of the MGF of the noise level estimate Z_{TM} becomes an easy task owing to the independency of its elements. Thus,

$$\Omega_{Z_{TM}}(s; N_i, L_i, U_i) = \prod_{j=1}^{N_T} \Omega_{E_j}(s; K_i, m_i, r_i) \Big|_s = (N_T - j + 1)s \ \& \ i=1,2 \tag{49}$$

Now, suppose that the lagging subset has r_1 cells from outlying target returns, $m_1=N/2-r_1$ ones from thermal background, L_1 trimmed samples from the lower end of its ordered-statistic, and U_1 censored cells from the upper end of its ordered-statistic. Similarly, assume that the leading subset has r_2 interfering cells, $m_2=N/2-r_2$ samples containing clutter, its associated ordered-statistic is clipping from its ends, where the lowest L_2 ordered cells are excised and U_2 largest ranked cells are nullified. Under these circumstances, the MGF's of their noise power level estimates, Z_1 & Z_2 , have the same form as that given by Eq.(49) after replacing its common parameters with their corresponding values for the leading and trailing subsets. Finally, the two noise level estimates are combined through the mean-level operation to constitute the final noise power estimate. Thus,

$$Z_f = \sum_{i=1}^2 Z_i \ \& \ \Psi_{Z_f}(s) = \frac{1}{S} \prod_{i=1}^2 \Omega_{Z_{TM}}(s; N_i, L_i, U_i) \ \& \ i=1,2 \tag{50}$$

Once the s -domain representation of the CDF of the resultant noise level estimate is formulated, the calculation of false alarm and detection probabilities of the tested processor can be easily achieved.

3.4 CA_OS & CA_TM Developed Schemes

In the CFAR world, some algorithms present better detection performance than others, where they provide a greater probability of detection for a given value of SNR, lower average decision threshold and as low as possible probability of false alarm deviations from the desired values. The difficulty in finding a solution based on a single CFAR algorithm to deal with diverse noise environments has led to the development of composite CFAR algorithm. The new category of the developed CFAR processors is designed to exploit the merits of the distinguished detectors. This category can be realized by parallel operation of these two types of CFAR schemes as Fig.(1) demonstrates. In this novel version of CFAR techniques, CA and either OS or TM schemes process their operations simultaneously and independently in such a way that the thresholding's constant T is common for achieving their own detection threshold against which the content of CUT is compared to independently decide the presence or absence of the searched target. The final decision about target presence is made in fusion center which is composed of an "AND" gate circuit. If both the input single decisions of the fusion center are positive, its final decision is the presence of the target in the tested sample. Otherwise, the fusion center's decision is negative and target is not at the location which corresponds to the CUT [11]. Owing to the independency of the single decisions about target presence of CA and TM candidates of the CATM resulting detector, the global false alarm and detection probabilities can be mathematically formulated as:

$$P_{fa}^{CA_TM(L,U)} = P_{fa}^{CA} P_{fa}^{TM(L,U)} \ \& \ P_d^{CA_TM(L,U)} = P_d^{CA} P_d^{TM(L,U)} \tag{51}$$

Since each one of the right hand side of Eq.(51) was previously calculated, the performance of the CATM novel model of CFAR schemes is completely analyzed.

4 Processor Performance Assessment

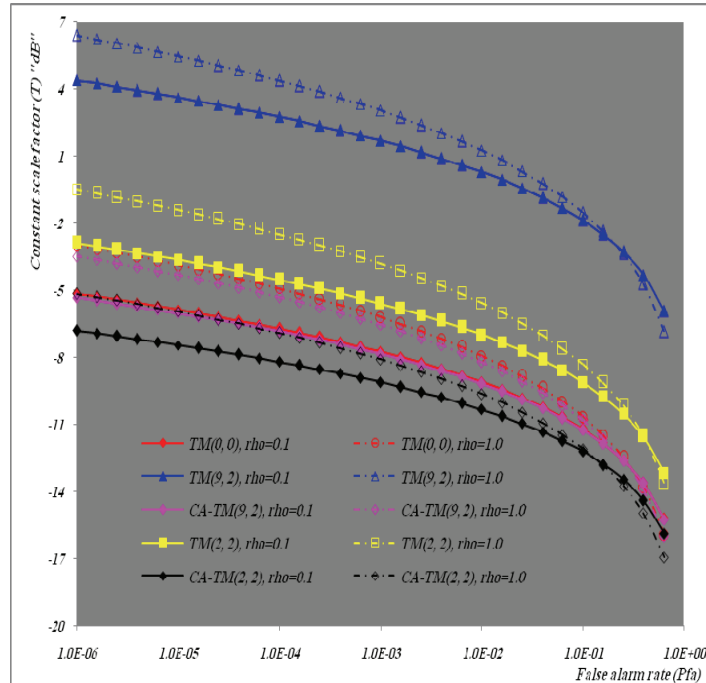


Figure 2. M -correlated sweeps thresholding constant, as a function of false alarm rate, of GTM family of CFAR schemes for $N=24$ and $M=3$

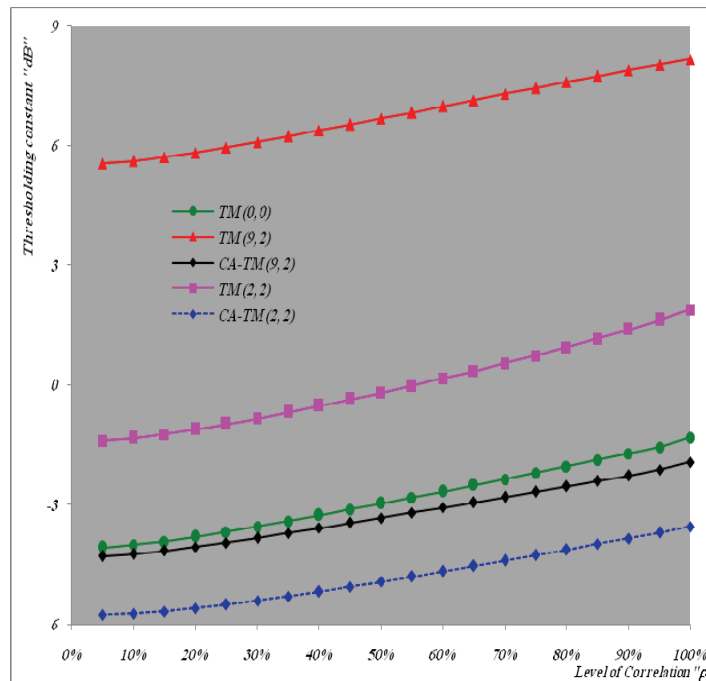


Figure 3. M -correlated sweeps thresholding constant, as a function of level of correlation, of GTM family of CFAR schemes when $N=24$ and $M=2$

To verify effectiveness of our analysis for the proposed CFAR algorithm, we carry out some numerical results to show to what extent the new category of CFAR processors can enhance the performance of their original versions. In all our numerical results, it is assumed that the reference window has a size of 24 cells and the designed rate of false alarm is 10^{-6} . We will present our numerical results in several categories of curves. The first category is concerned with plotting the variation of T for the tested detectors. This category includes Figs.(2-3). Fig.(2) depicts the changes of the thresholding constant as a function of the false alarm rate when three consecutive sweeps ($M=3$) are either weakly ($\rho=0.1$) or strongly ($\rho=1.0$) correlated. For simplicity, it is convenient to refer each one of the underlined detectors with its equivalent representation in TM technique. The displayed results show that as the false alarm rate increases, the constant scale factor decreases. Additionally, as the correlation among the sweeps becomes strengthened, the T value raises to reply the same rate of false alarm. Moreover, the TM(9,2), which represents OS(10) requires the highest T values whilst the modified version CA_TM(2,2) needs the lowest to satisfy the same probability of false alarm. The schemes TM(0,0), which denotes the CA technique, along with the standard TM(2,2) and the derived scenario CA_TM(9,2) request intermediate vales for the weighting factor T to guarantee the designed rate of false alarm. This ordering of the examined CFAR algorithms is clearly evident from the results of Fig.(3), which is concerned with the same characteristic and its variation with the strength of correlation (ρ) among the consecutive pulses.

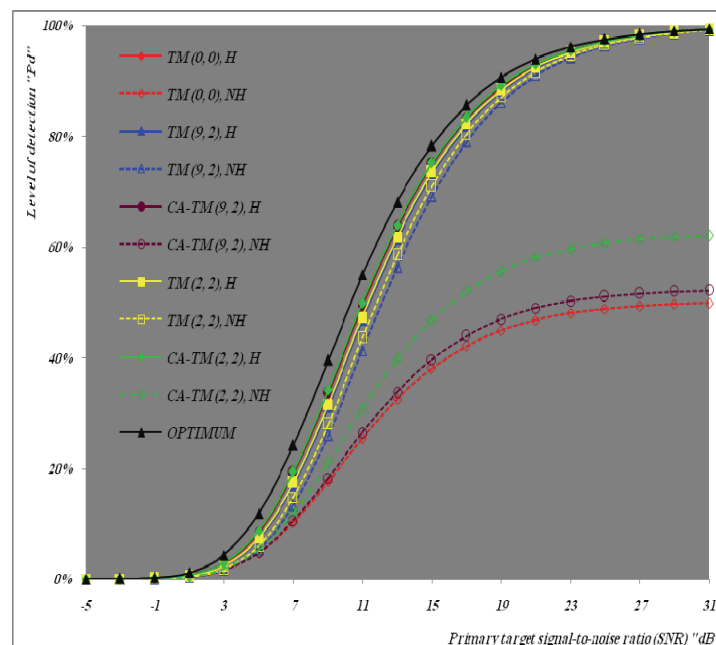


Figure 4. M -correlated sweeps detection performance of GTM family of CFAR schemes when $N=24$, $M=2$, $\rho=0$, $r_1=r_2=1$, and $P_{fa}=10^{-6}$

The second category of curves is devoted to the processor detection performance in the absence "H" as well as in the presence "NH" of spurious targets when the primary and the secondary interfering targets have the same signal strength ($\text{INR}=\text{SNR}$) and their consecutive sweeps have the same correlation strength. This performance represents the principle figure of merit in distinguishing the various forms of signal detectors. For comparison, the optimum (Naymann-Pearson) performance is attached to the candidates of this category. This category comprises Figs.(4-11). Fig.(4) depicts the processor performance for de-correlated ($\rho=0$) two consecutive sweeps ($M=2$) in ideal ($r_1=r_2=0$) and when there are two reference cells contaminated with outlying target returns ($r_1=r_2=1$). The curves of this figure are parametric in the CFAR processor along with the state of operating environment. It is shown that the new versions CA_TM(2,2) and CA_TM(9,2) have the top homogeneous performance whilst the standard TM(9,2) scheme gives the worst. In multi-target situation, the conventional TM(2,2) scenario has the highest performance whilst the TM(0,0) algorithm offers the lowest. It is evident that the modified forms precede the CA procedure in their homogeneous performance and moderately improve

its multi-target behavior. To show the effect of increasing the number of sweeps on the processor performance, Fig.(5) repeats the same characteristic for the underlined detectors when M is augmented from 2 to 4 taking into account that all the other parameters are held unchanged. As this plot demonstrates, increasing the number of sweeps enhances the detection performance of the CFAR algorithm either it operates in ideal or target multiplicity environment.

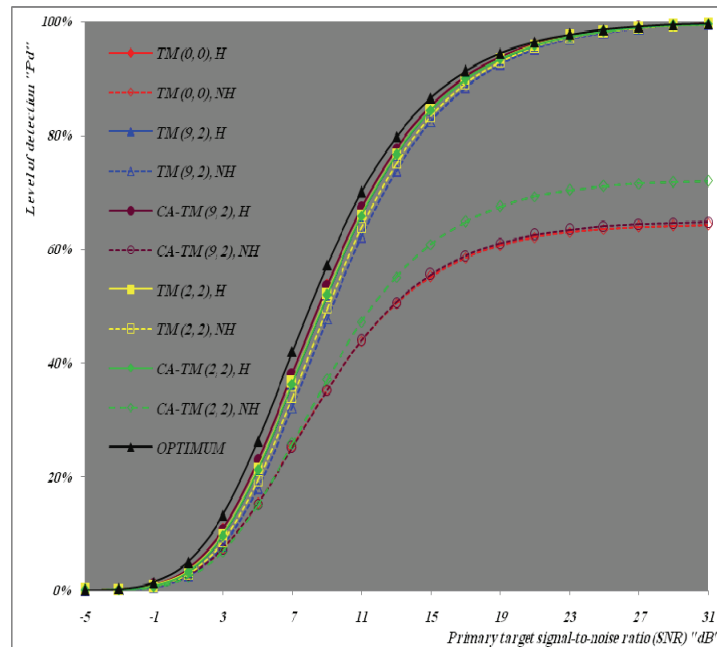


Figure 5. M -correlated sweeps detection performance of GTM family of CFAR schemes when $N=24$, $M=4$, $\rho=0$, $r_1=r_2=1$, and $P_{fa}=10^{-6}$

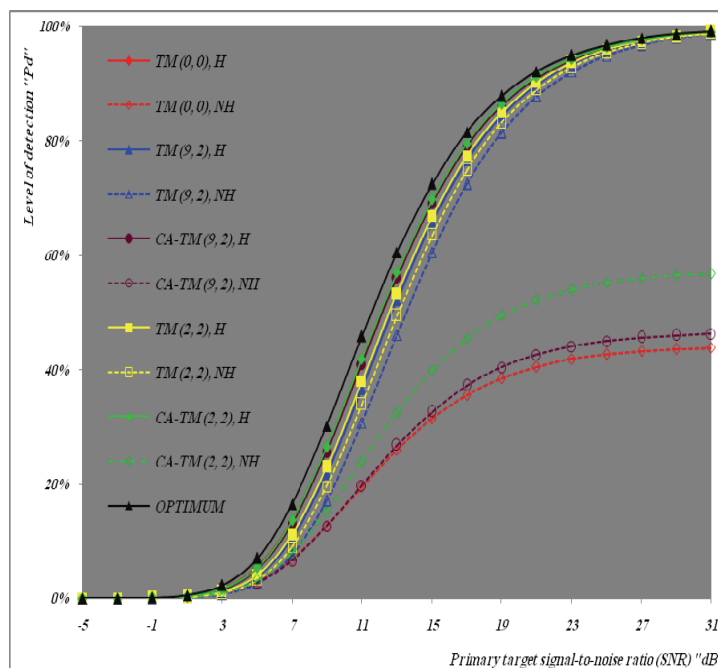


Figure 6. M -correlated sweeps detection performance of GTM family of CFAR schemes when $N=24$, $M=2$, $\rho=0.50$, $r_1=r_2=1$, and $P_{fa}=10^{-6}$

To show to what extent the correlation among the consecutive sweeps worsens the processor performance, Figs.(6 & 7) replicate the same characteristics of Figs.(4 & 5) in the case where the successive pulses have 50% correlation. In this situation, the processor behavior remains unchanged except that the detection probability attains lower values in comparison with its values in de-correlated case.

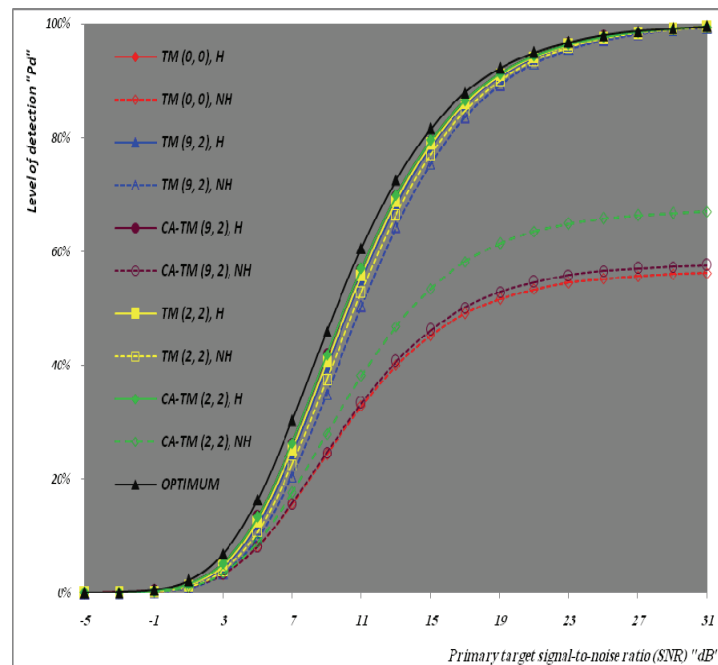


Figure 7. M -correlated sweeps detection performance of GTM family of CFAR schemes when $N=24$, $M=4$, $\rho=0.50$, $r_1=r_2=1$, and $P_{fa}=10^{-6}$

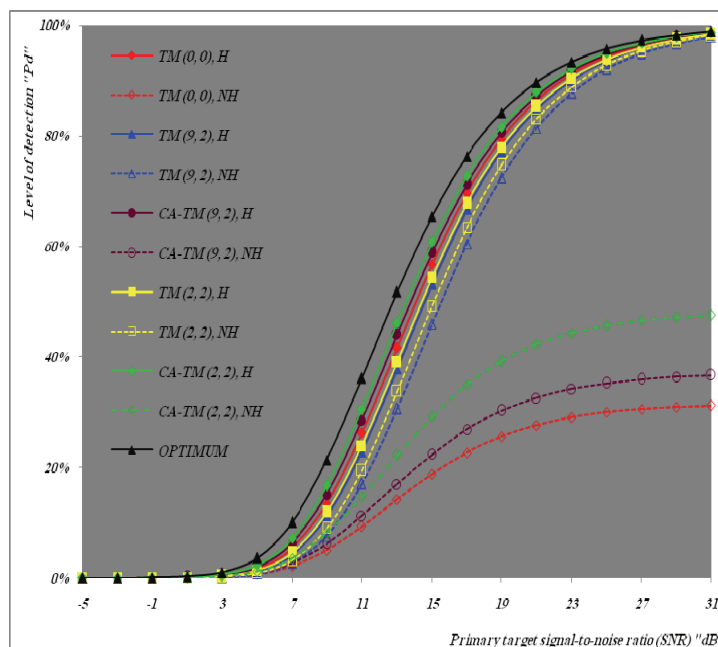


Figure 8. M -correlated sweeps detection performance of GTM family of CFAR schemes when $N=24$, $M=2$, $\rho=1.0$, $r_1=r_2=1$, and $P_{fa}=10^{-6}$

The next two scenes, Figs.(8 & 9), are the similar replicas of Figs.(4 & 5) when the consecutive sweeps are fully correlated. It is evident that the processor performance becomes more worsen in comparison with their corresponding case in Figs.(6 & 7). A special interest is given to the performance of the novel versions to see their reaction against correlated sweeps in ideal situation of operation. Figs.(10 & 11) depict the detection performance of CA_OS(10) and CA_TM(2, 2) models when 2 or 4 consecutive pulses are incoherently integrated. Additionally, the processor behavior, as a function of the strength of correlation among the successive sweeps, is presented to see to what extent the correlation can degrade the detection process of the underlined strategies.

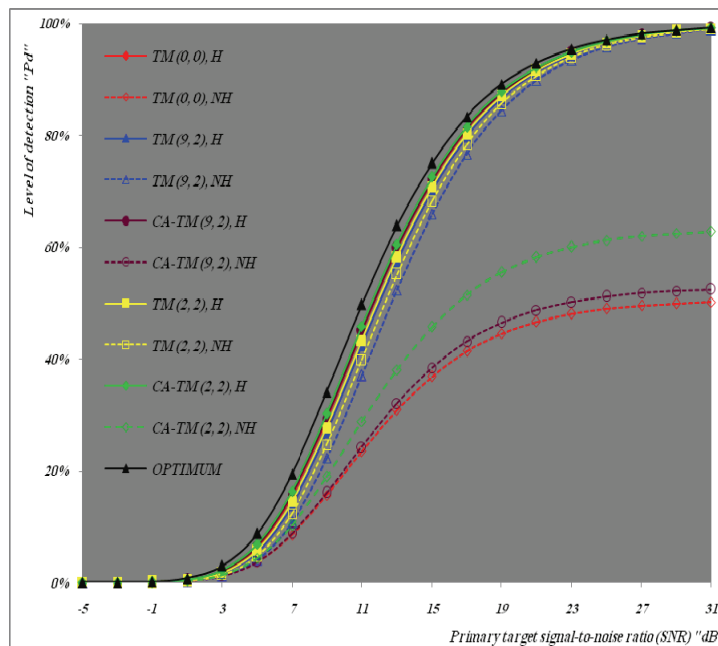


Figure 9. M -correlated sweeps detection performance of GTM family of CFAR schemes when $N=24$, $M=4$, $\rho=1.0$, $r_1=r_2=1$, and $P_{fa}=10^{-6}$

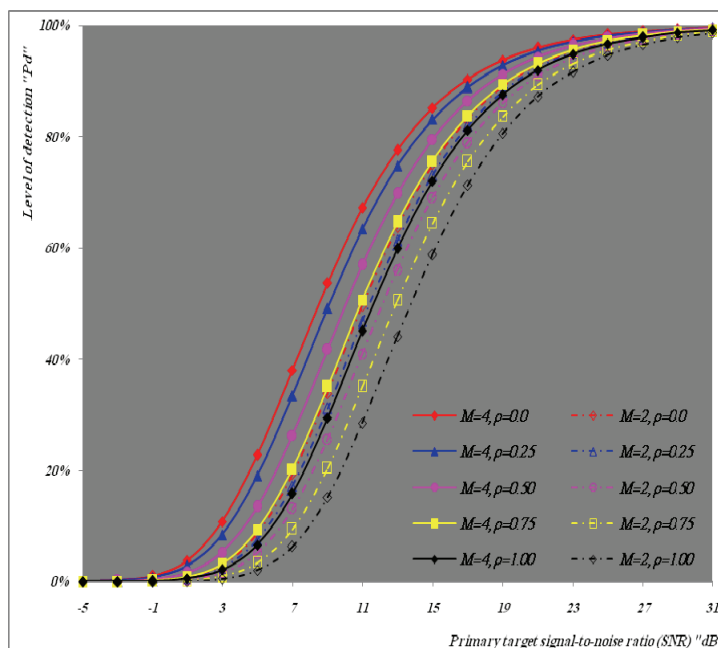


Figure 10. M -correlated sweeps homogeneous detection performance of CA_OS(10) scheme when $N=24$ & $P_{fa}=10^{-6}$

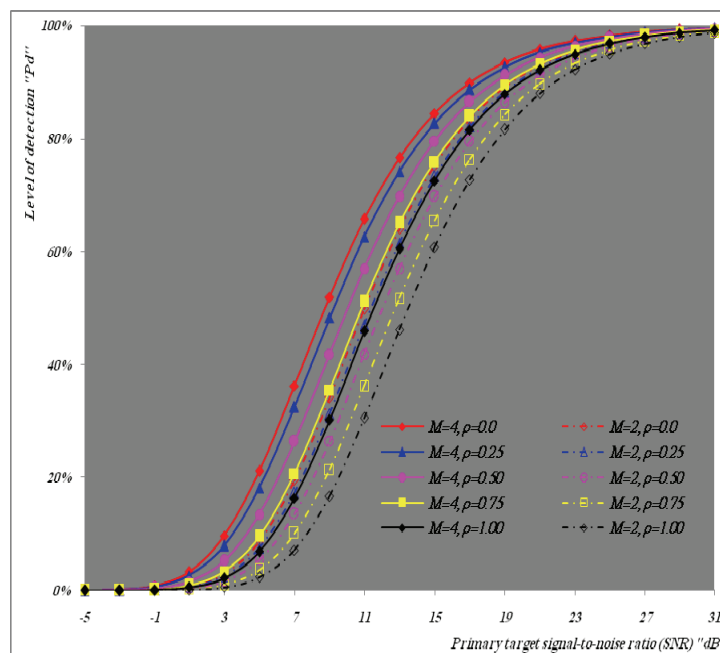


Figure 11. M -correlated sweeps homogeneous detection performance of CA_TM(2, 2) algorithm when $N=24$ & $P_{fa}=10^{-6}$

Clearly, the displayed results of these plots demonstrate that as the correlation among the consecutive sweeps becomes strengthen, the detection level tends to be degraded. Moreover, for the same level of correlation, the detection probability enhances as the number of sweeps increases.

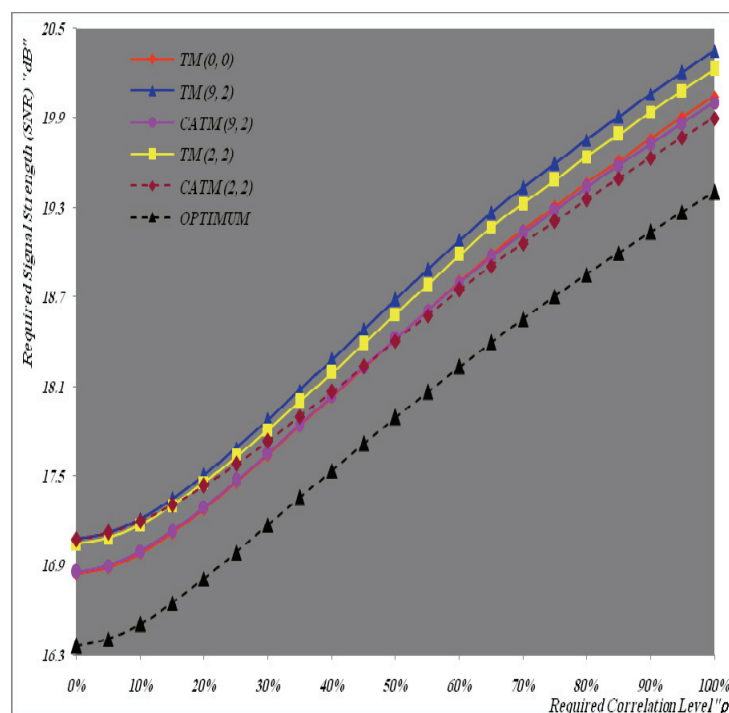


Figure 12. M -correlated sweeps required SNR to achieve a homogeneous detection level of 90% of GTM family of CFAR processors when $N=24$, $M=4$, and $P_{fa}=10^{-6}$

An another important category of curves is that associated with the needed signal strength to reply a detection level of 90%, given that the operating environment is ideal and the false alarm rate is held

constant. This category contains Fig.(12). In this figure, the required SNR is drawn against the correlation strength (ρ) among four ($M=4$) successive pulses when the tested processor is designed to guarantee a 10^{-6} rate of false alarm. For the sake of comparison, the optimum detector is added to the candidates of this plot.

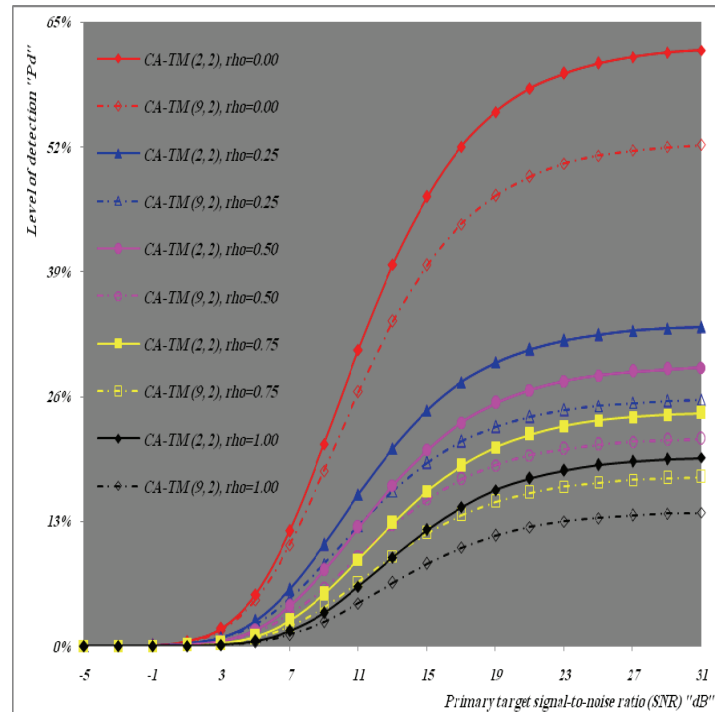


Figure 13. M -correlated sweeps multi-target detection performance of CA-GTM family for $N=24$, $M=2$, $r_1=r_2=1$, and $P_{fa}=10^{-6}$

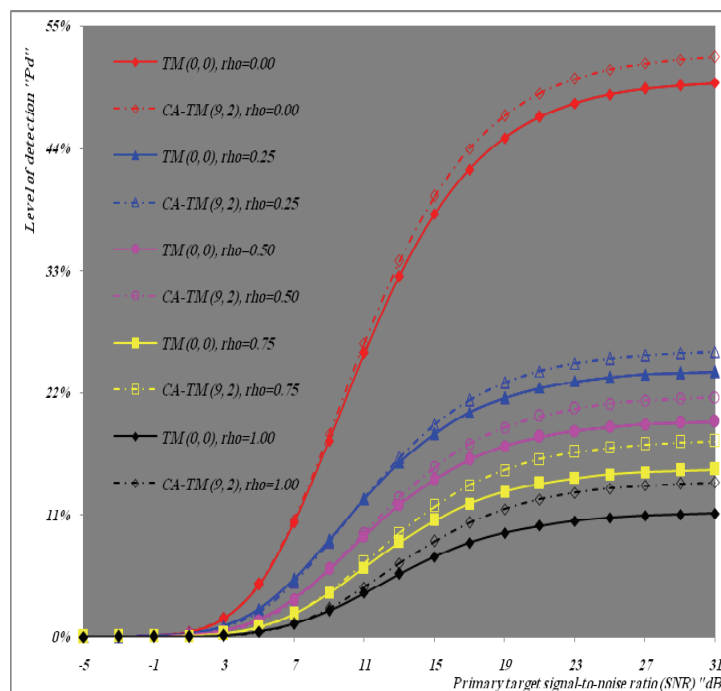


Figure 14. M -correlated sweeps multi-target detection performance of GTM family for $N=24$, $M=2$, $r_1=r_2=1$, and $P_{fa}=10^{-6}$

As the displayed results demonstrate, it is obvious that the standard CA and the modified CA_OS(10) detectors present the highest performance when the consecutive sweeps are weakly correlated. As the correlation becomes strengthened, the new model CA_TM(2, 2) gives the highest performance, which is the nearest one to that of the optimum procedure, whilst the conventional OS(10) algorithm possesses the worst one. Furthermore, any detection scheme needs more strengthened signal, to reply the specified detection level, as the successive pulses become strongly correlated.

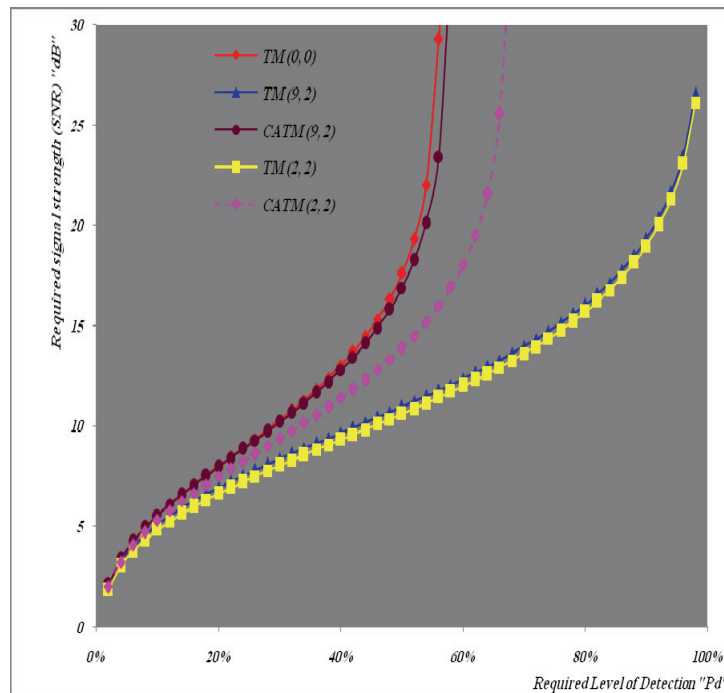


Figure 15. M -correlated sweeps multi-target required SNR, to achieve a needed detection level, of GTM family when $N=24$, $M=4$, $\rho=0.5$, $r_1=r_2=1$, and $P_{fa}=10^{-6}$

Now, it is of importance to see to what extent the new versions can improve the reaction of the ordinary CA processor against the presence of outlying targets among the contents of the reference channels. This category of curves includes Figs.(13 & 14). Fig.(13) illustrates the detection performance of the novel models CA_OS(10) and CA_TM(2, 2) for double ($M=2$) correlated pulses with different correlation strength when the reference channels are contaminated with two ($r_1=r_2=1$) spurious target returns of the same signal strength ($INR=SNR$) as the primary target. It is interesting to note that the full scale of the y-axis is 0.65 instead of unity. It is shown that the new version CA_TM(2, 2) gives always a performance that is superior to that of CA_OS(10) model under the same correlation strength. On the other hand, Fig.(14) is devoted to compare the performance of CA_OS(10) with the traditional CA detector under the same conditions as those presented in Fig.(13). The exhibited results show the superiority of the modified form over the normal CA processor.

Finally, since the derived versions aren't able to reply any detection level in multiple-target environment, it is of interesting to calculate the SNR requested to satisfy a given level of detection for a specified correlation among the consecutive sweeps. Fig.(15) presents such sort of detection performance. It traces the signal strength, that is required for the detection probability to reach a given level when four ($M=4$) successive pulses have 50% strength of correlation, for the modified as well as the original detectors. It is clearly that the novel versions can verify a given detection level till a specified value beyond which they haven't the ability to reply any further level. Additionally, the cutoff level of CA_TM(2, 2) is higher than that of CA_OS(10) which is in turn larger than that of the CA algorithm. On the other hand, the standard OS(10) and TM(2, 2) schemes are the only ones that are able to respond any detection level.

5 Conclusions

This paper deals with the problem of detection of a moving target against clutter background. It was analyzed the performance of a radar signal processor that consists of a non-recursive MTI followed by a square-law integrator and a new version of adaptive circuit detection; the operation of which is based on the hybrid combination of CA and OS/TM algorithms. The presence of MTI in the operating circuit complicates its analysis since the output sequence of MTI is correlated even its input sequence is not. This correlation is the main reason for the processor performance degradation. We have given a detailed analysis of the detection performance of the new developed versions along with their original schemes in multi-target situations, when these detection strategies processing data that are fitted to them through such type of MTI. The numerical results demonstrate that the novel versions ameliorate the performance of the ordinary CA mechanism when the operating environment is free-of or contaminated-with interferer returns. For each one of the underlined detectors, the detection performance enhances as the correlation among successive pulses decreases or the number of pulses increases. As a conclusion from the displayed results, we state that increasing the chance for the tested target to be detected means that the correlation among consecutive sweeps must be as small as possible and the number of incoherently integrated pulses will be augmented, if possible, owing to the lower threshold values that are acquired by the strategy of integration. However, increasing the number of sweeps leads to increasing the complexity of the detector structure along with increasing the processing time which is the most important parameter in the radar operation.

References

1. Rickard, J. T. & Dillard, G. M., "Performance of an MTI followed by incoherent integration for nonfluctuating signals", IEEE International Radar Conference, pp. 194-199, 1980.
2. El Mashade, M. B., "Detection performance of the trimmed-mean CFAR processor with noncoherent integration", IEE Proc. Radar, Sonar Navig., Vol. 142, No. 1, pp.18-24, February 1995.
3. El Mashade, M. B., "Monopulse detection analysis of the trimmed mean CFAR processor in nonhomogeneous situations", IEE Proc. Radar, Sonar Navig., Vol. 143, No. 2 , pp.87-94, April 1996.
4. El Mashade, M. B., "Performance analysis of OS family of CFAR schemes with incoherent integration of M-pulses in the presence of interferers", IEE Proc. Radar, Sonar Navig., Vol.145, No.3, (June 1998), pp. 181-190.
5. El Mashade, M. B., "Partially correlated sweeps detection analysis of mean-level detector with and without censoring in nonideal background conditions", Int. J. Electron. Commun. (AEÚ), Vol.53, No.1, (Feb. 1999), pp. 33-44.
6. El Mashade, M. B., "Detection analysis of CA family of adaptive radar schemes processing M-correlated sweeps in homogeneous and multiple-target environments", Signal Processing "ELSEVIER", Vol.80, (Aug. 2000), pp. 787-801.
7. El Mashade, M. B., "Analysis of Cell-Averaging Based Detectors for χ^2 Fluctuating Targets in Multitarget Environments", Journal of Electronics (China), Vol.23, No.6, (November 2006), pp. 853-863.
8. El Mashade, M. B., "M-correlated sweeps performance analysis of adaptive detection of radar targets in interference-saturated environments", Ann. Telecommun., Vol. 66, pp. 617-634, 2011.
9. W. Q. Wang, "Radar Systems: Technology, Principals and Applications", Nova Science Publishers, Inc, 2013.
10. El Mashade, M. B., "Analysis of adaptive detection of moderately fluctuating radar targets in target multiplicity environments", Journal of the Franklin Institute 348 (2011), pp. 941-972.
11. Dejan Ivković, Milenko Andrić and Bojan Zrnić, "A New Model of CFAR Detector", Frequenz 2014; 68(3-4): 125 - 136.
12. Amritakar Mandal & Rajesh Mishra, "An Adaptive Clutter Suppression Technique for Moving Target Detector in Pulse Doppler Radar", Radioengineering, Vol. 23, No. 1, April 2014, pp.84-95.
13. El Mashade, M. B., "Adaptive Detection Enhancement of Partially-Correlated χ^2 Targets in an Environment of Saturated Interference", Recent Advances in Electrical & Electronic Engineering, Vol.9, No.2, pp.1-21, 2016.
14. El Mashade, M. B., "Heterogeneous Performance Evaluation of Sophisticated Versions of CFAR Detection Schemes", Radioelectronics and Communications Systems, 2016, Vol. 59, No. 12, pp. 536-551.
15. El Mashade, M. B., "Heterogeneous Performance Analysis of the New Model of CFAR Detectors for Partially-Correlated χ^2 -Targets", Journal of Systems Engineering and Electronics, Vol. 29, No. 1, pp. 1-17, Feb. 2018.